NEURAL NETWORK-DRIVEN INSIGHTS INTO UTERINE SUSPENSORY TISSUE BIOMECHANICS IN WOMEN WITH PELVIC ORGAN PROLAPSE

Hui Wang (1,2,3), Zhuowei Xue (4), Chenxin Zhang (1,2,3), Fei Feng (5), Chengsheng Huang (4), Da He (5), Xinyi Wang (5), Jianwei Zuo (1,2,3), Qingkai Wu* (4), Jiajia Luo* (1,2,3)

(1) Institute of Medical Technology, Peking University Health Science Center, Beijing, China

(2) Institute of Advanced Clinical Medicine, Peking University, Beijing, China.

(3) Biomedical Engineering Department, Peking University, Beijing, China

(4) Department of Obstetrics and Gynecology, Shanghai Jiao Tong University Affiliated Sixth People's Hospital, Shanghai, China

(5) University of Michigan-Shanghai Jiao Tong University Joint Institute, Shanghai Jiao Tong University, Shanghai, China

Preferred presentation: Oral
Area Topic: AI
Controlled Trial: No
Systematic review: No
IRB: approved
Already presented: No

Introduction:

The uterine suspensory tissue (UST) consisting of the cardinal ligament (CL) and the uterosacral ligament (USL), is thought to play an important role in maintaining pelvic structural stability and resisting pelvic organ prolapse (POP). Understanding their biomechanics is crucial to comprehend the mechanisms of the occurrence of POP. While various constitutive models have been proposed in the past to describe the mechanical properties of biological tissues, the selection of the most suitable constitutive model for UST still represents an unresolved challenge.

Objective:

We aimed to employ a neural network (or deep learning model) for autonomous discovery of the optimal constitutive model for UST and quantification of the biomechanical properties of UST in women with POP.

Methods:

Six women with POP scheduled for surgery were selected from an ongoing POP research with the approval of the IRB. We adopted a constitutive artificial neural network (CANN) to autonomously discover the constitutive model of UST. The specific network structure was illustrated in Figure 1. This network ensures that the obtained constitutive model satisfies physical laws and provides clear physical interpretations for each weight. The UST of these patients were measured in vivo using our developed measurement device. A biomechanical model was established based on MRI scans to determine the stretch and nominal uniaxial stress for both the CL and the USL. Each participant's data for each ligament consisted of 18 pairs, with 15 pairs used for training and 3 pairs used for testing. The network was constructed using Keras-2.9.0 and trained for 5000 epochs to ensure convergence of the mean squared error (MSE) loss function. The autonomous discovery of

constitutive models is achieved through network training in this study, with model performance quantitatively evaluated using the coefficients of determination (R^2). To demonstrate the method's effectiveness, we compared its fitting results with a typical Mooney-Rivlin biomechanical constitutive model.

Results:
The parameters of the constitutive model discovered by the trained network are shown in Table 1 for both CL and USL. Moreover, the network autonomously discovers the constitutive model, as shown in Figure 2, and accurately fits the experimental data. Furthermore, Figure 3 demonstrates that the autonomously discovered constitutive model through the network achieves superior fitting performance in contrast to the Mooney-Rivlin model.

Conclusions:
In this study, a neural network-based autonomous discovery approach was used to construct the constitutive model for POP patients with UST, ensuring it conforms to physical laws and provides interpretable weights. This approach outperforms typical biomechanical constitutive models like the Monney-Rivlin model in terms of fitting, making it a valuable tool for identifying UST's biomechanics more accurately and furthering our understanding of its mechanisms responsible for POP's occurrence with finite element simulation.

Disclosure:

Keywords: Pelvic organ prolapse, Deep learning, Uterine suspensory tissue, Biomechanics, Constitutive model

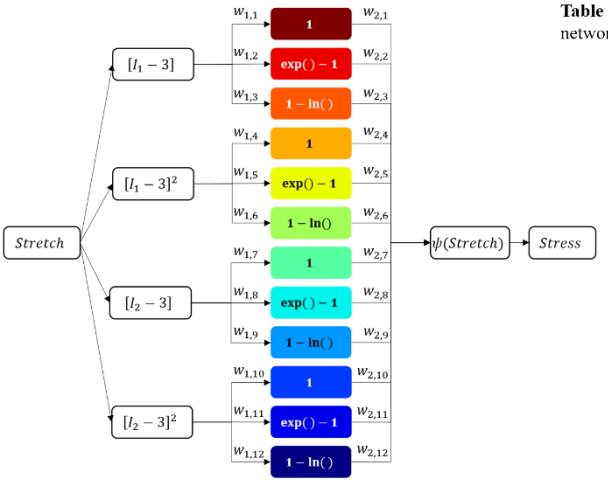

Figure 1: CANN structure

Table 1: Parameter values of the constitutive model discovered by the trained network for CL and USL: mean and standard deviation analysis of 6 patients

	Cardinal Ligament		Uterosacral Ligament	
	$w_{1,\cdot}$	$w_{2,\cdot}$	$w_{1,\cdot}$	$w_{2,\cdot}$
$w_{\cdot,1}$	1.784±0.641	0.641±1.666	0.852±0.943	0.696±0.841
$w_{\cdot,2}$	0.786±1.174	1.174±1.215	0.284±0.395	0.695±0.397
$w_{\cdot,3}$	1.314±0.955	0.955±1.663	1.991±2.385	0.774±0.512
$w_{\cdot,4}$	0.382±0.095	0.095±0.478	0.399±0.564	0±0.001
$w_{\cdot,5}$	1.216±1.027	1.027±2.159	0.08±0.18	0.161±0.234
$w_{\cdot,6}$	1.533±0.637	0.637±3.695	0.514±0.631	0.013±0.031
$w_{\cdot,7}$	2.411±2.139	2.139±1.42	2.406±2.056	1.528±1.31
$w_{\cdot,8}$	1.465±2.196	2.196±1.271	1.029±0.808	2.114±0.817
$w_{\cdot,9}$	1.481±0.896	0.896±1.677	1.132±1.711	0.643±0.932
$w_{\cdot,10}$	0.157±0.076	0.076±0.248	0.117±0.181	0.176±0.432
$w_{\cdot,11}$	0.218±0.715	0.715±0.334	0.134±0.319	0.106±0.134
$w_{\cdot,12}$	0.64±0.214	0.214±0.685	0.191±0.382	0.077±0.187

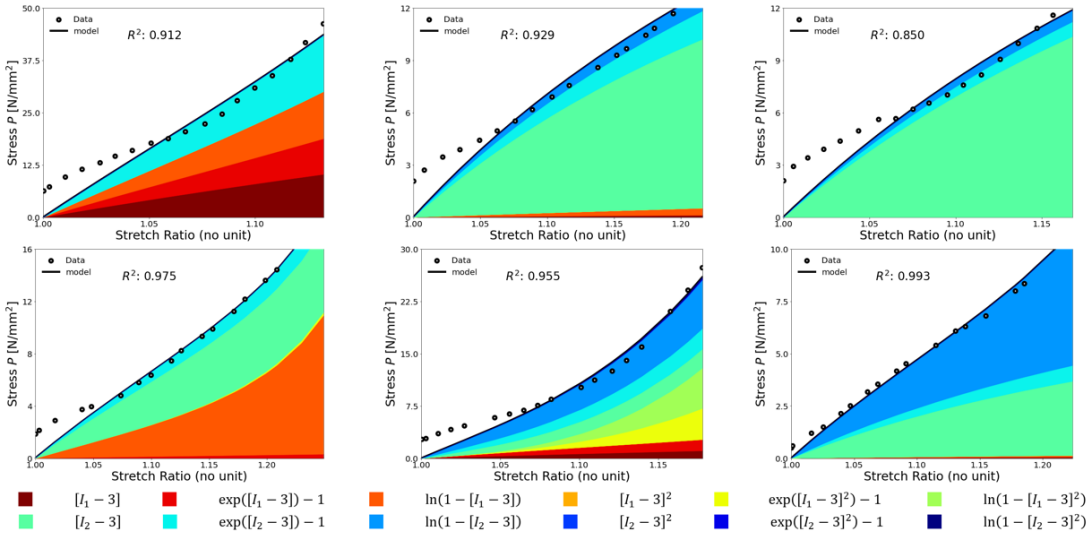

(a)

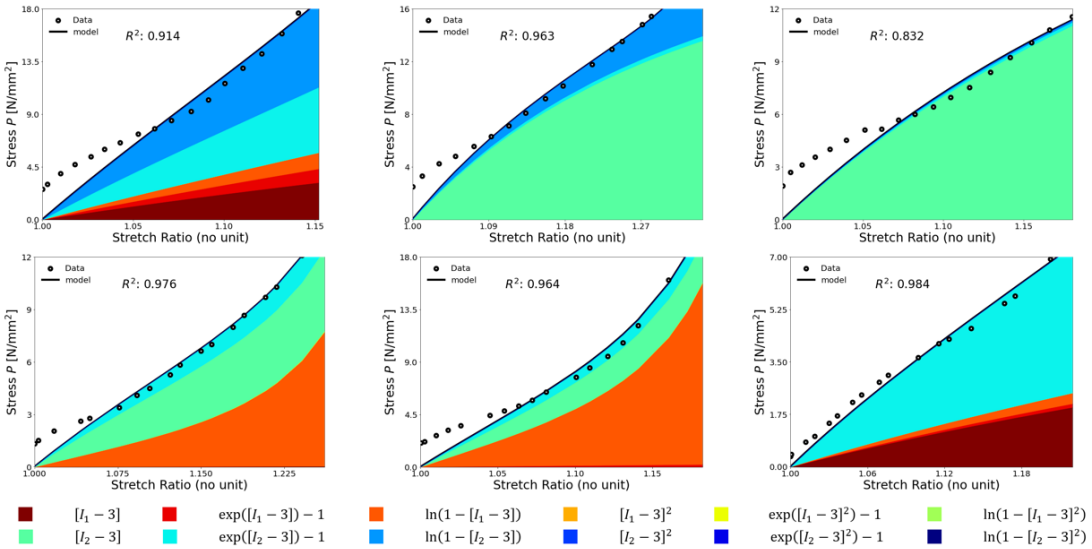

(b)

Figure 2: Model and parameter discovery for CL (a) and USL (b). Dots illustrate the experimental data, and the solid black lines illustrate the fit results. Color-coded areas highlight the 12 contributions to each item from Figure 1.

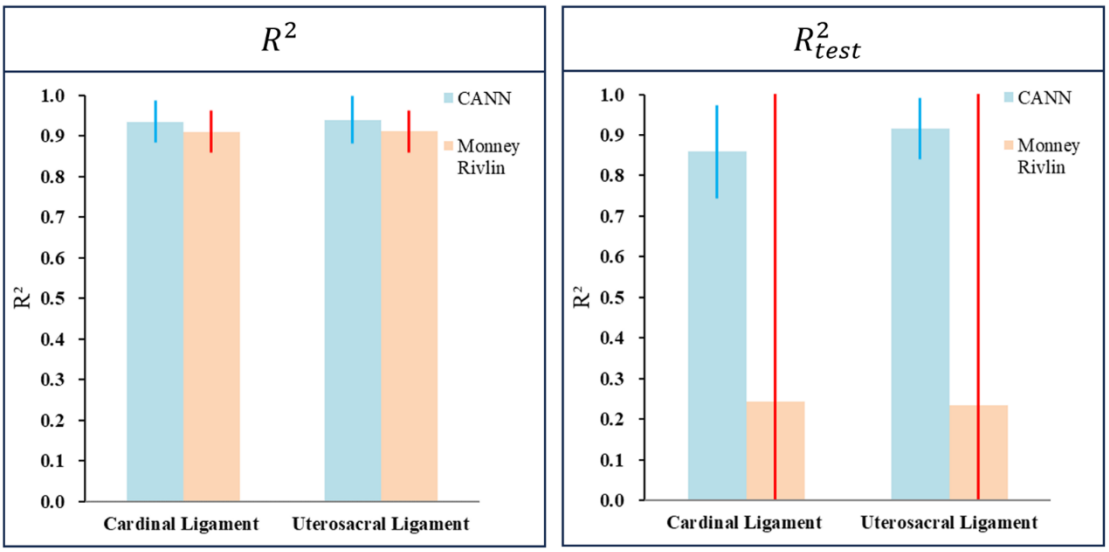

Figure 3: Goodness of fit for CANN and Mooney-Rivlin models: full dataset and testing set results.